UDK 551.243, 553.7 doi.org/10.30730/2541-8912.2019.3.4.345-363

Characteristics of tectonic activity phases along The Cao Bang – Tien Yen fault zone, Tien Yen – Lang Son section, Northeastern part, Vietnam

© 2019 *Truong Thanh Phi*[1], *Renat B. Shakirov**[2], *Nadezhda S. Syrbu***[2]

[1]*Hanoi University of Natural Resourses and Environment, Vietnam*
[2]*V.I. Il'ichev Pacific Oceanological Institute, FEB RAS, Vladivostok, Russia*
**E-mail: ren@poi.dvo.ru*
***E-mail: syrbu@poi.dvo.ru*

Abstract. The Cao Bang – Tien Yen (CB-TY) fault zone, Tien Yen – Lang Son (TY-LS) section is about 100 km long, running in the NW-SE direction, the northeastern part of the Red River fault zone. The field survey is conducted at 21 locations, including the description of lithological characteristics, fracture orientation measurement, stratigraphic displacement, and the evidence of striation motion on the fault surface. The analytical results of 59 striations on the fault surface along the CB-TY fault zone, TY-LS section identified that the lateral strike-slip stress states with the four compression phases E-W, NE-SW, NW-SE and N-S. From evidences obtained in the field, together with the comparison of previous studies, the main tectonic phases are arranged in the order of directions: 1) NW-SE; 2) E-W; 3) NE-SW and 4) N-S. In particular, the first compression phase of the NW-SE direction severely destroyed the old rocks of the Jurassic age and earlier, encountered at many survey locations along the CB-TY fault zone, TY-LS section; the second compression phase of the E-W direction occurred during the Cenozoic period, caused the left displacement of the Red River fault zone in the Oligocene-Miocene period and the left motion along the CB-TY fault zone formed the Neogen sedimentary basins: Cao Bang, That Khe, Lang Son, Na Duong; the third compression phase of NE-SW direction occurred during the Mid-late Miocene, caused a tectonic inversion of the NW-SE faults in the northern part of the Red River basin, which are located in the southeast area of the CB-TY fault zone; the final compression phase of the N-S direction, occurred during the Pliocene-Quaternary period, caused the right motion along the CB-TY fault zone and the Red River fault zone.

Keywords: CB-TY fault zone, Red River fault zone, Cao Bang basin, Neogene Na Duong basin, TY-LS section, thermal springs.

For citation: Truong Thanh Phi, Shakirov R.B., Syrbu N.S. Characteristics of tectonic activity phases along The Cao Bang – Tien Yen fault zone, Tien Yen – Lang Son section, Northeastern part, Vietnam. *Geosystems of Transition Zones.* 2019, vol. 3, no. 4, pp. 345–363. (In English, abstract Russian) https://doi.org/10.30730/2541-8912.2019.3.4.345–363

Характеристики фаз тектонической активности вдоль зоны разлома Цхао Банг – Ти Иен, разрез Ти Иен – Ланг Сон, северо-восточная часть, Вьетнам

Чон Тхань Фи[1], ***Р.Б. Шакиров****[2], ***Н.С. Сырбу*****[2]

[1]*Ханойский университет природных ресурсов и окружающей среды, Вьетнам*
[2]*Тихоокеанский океанологический институт им. В.И. Ильичева ДВО РАН, Владивосток, Россия*
**E-mail: ren@poi.dvo.ru*
***E-mail: syrbu@poi.dvo.ru*

Реферат (расширенный). Разлом Цхао-Банг – Ти-Иен, разрез Ти-Иен – Ланг-Сон имеет длину около 100 км, он простирается в северо-западном – юго-восточном направлении в северо-восточной части разломной зоны Красной Реки. Полевые исследования проводились на 21-м участке. Они включали описание литологических характеристик, измерение ориентации трещин, стратиграфическое смещение и оценку признаков движения на поверхности разлома. Результаты анализа

59 полос скольжения на поверхности разлома вдоль зоны Цхао-Банг – Ти-Иен, разреза Ти-Иен – Ланг-Сон показали, что боковое ударно-скользящее напряжение находится в состоянии сжатия по четырем фазам в направлениях В-З, СВ-ЮЗ, СЗ-ЮВ, С-Ю. По полученным данным в сравнении с предыдущими исследованиями были выделены основные направления тектонических движений: 1) СЗ-ЮВ; 2) В-З; 3) СВ-ЮЗ и 4) С-Ю. В частности, первая фаза сжатия СЗ-ЮВ простирания значительно нарушила древние породы эпохи юрского периода и более ранних. Такие участки встречаются во многих местах обследования вдоль зоны разлома Цхао-Банг – Ти-Иен, разреза Ти-Иен – Ланг-Сон. Вторая фаза сжатия В-З простирания произошла в кайнозойский период, вызвала левое смещение разломной зоны Красной Реки в олигоцен-миоценовом периоде и образовала осадочные неогеновые Цхао Банг, Тат Кхе, Ланг Сон, На Дуонг вдоль зоны разлома Цхао-Банг – Ти-Иен. Третья фаза сжатия СВ-ЮЗ простирания произошла во время среднего–позднего миоцена, вызвала тектоническую инверсию разломов СЗ-ЮВ направления в северной части бассейна Красной Реки, которые расположены в юго-восточной зоне разлома Цхао-Банг – Ти-Иен. Заключительная фаза сжатия С-Ю простирания, происходившая в плиоцен-четвертичный период, обусловила правое движение вдоль зоны разлома Цхао-Банг – Ти-Иен и разломной зоны Красной Реки.

В районе исследований на участке разлома Цхао-Банг – Ти-Иен и разломной зоны Красной Реки за период 2017–2019 гг. было опробовано 28 термальных источников, взято более 50 проб воды для газогеохимического и изотопного анализа. Пробы анализировали на содержание углеводородных газов (УВГ), N_2, O_2, CO_2, Не и H_2, проводили расчет потока метана в атмосферу с поверхности источников. Наиболее важным результатом исследований стало установление взаимосвязи режима термальных источников, термогенной газовой компоненты с геологической структурой Северного Вьетнама.

Основываясь на тектонических данных и результатах анализов химического состава природных газов, можно утверждать, что выходы термальных вод в районе северо-западного Вьетнама приурочены к активным зонам разломов. Смещения вдоль основных разломных зон способствуют увеличению проницаемости, облегчают продвижение тепла и термогенных газов к поверхности. Во всех исследованных термальных источниках, расположенных в зоне влияния рифта Красной Реки и разлома Цхао-Банг – Ти-Иен, обнаружены повышенные концентрации водорода (5900 нл/л), гелия (до 4252 нл/л), углекислого газа (до 72 %), метана (до 137 776 нл/л), что свидетельствует о геодинамической активности в районе исследований и о возможной поставке глубинного флюида по сверхглубоким проницаемым зонам.

Выходы термальных вод на северо-западе приурочены к системам разломов СЗ-ЮВ простирания: Сонг Да, Тхуан Чау, Сонг Хонг и Сонг Чау. Источники, расположенные в провинции Лао Кай, находятся в гранитном массиве Фансипан. Исследуемые источники в районе Северной Вьетнамской низменности (Ба Ви и Ким Бой) были обнаружены при разведочном бурении. В провинции Хоа Бинх (дельта Красной Реки), находящейся в отдаленных пригородах Ханоя к юго-востоку от его центра, зафиксированы концентрации углекислого газа в воде до 42 %. Также рассчитан поток метана с поверхности источника в атмосферу – 593 мкмоль/сутки.

В соседней провинции Фу То также зафиксированы высокие концентрации углекислого газа в воде – до 50 %. Концентрации метана повышены и достигают 2150 нл/л. Поток метана в атмосферу составляет 100–400 мкмоль/сутки. Температура воды одного из источника доходила до 43 °С.

Проблема газогеохимического режима термальных, карстовых и подземных вод Северного Вьетнама тесно связана с комплексной оценкой углеводородного потенциала и геоэкологической обстановки района рифта Красной Реки. В районе исследований распространены термальные источники, газовый состав которых известен в самых общих чертах. Между тем макро- и микрогазовые компоненты (углеводородные газы, кислород, азот, водород, гелий, углекислый газ и др.) содержат информацию о генезисе проницаемых систем земной коры, глубинных источниках газов, их влиянии на геохимию окружающих ландшафтов и других особенностях связи сквозных процессов литосфера–гидросфера–атмосфера.

Ключевые слова: разлом Цхао Банг – Ти Иен, разломная зона Красной Реки, бассейн Цхао Банг, бассейн На Дуонг, разрез Ти Иен – Ланг Сон, термальные источники.

Для цитирования: Чон Тхань Фи, Шакиров Р.Б., Сырбу Н.С. Характеристики фаз тектонической активности вдоль зоны разлома Цхао Банг – Ти Иен, разрез Ти Иен – Ланг Сон, северо-восточная часть, Вьетнам. *Геосистемы переходных зон.* 2019. Т. 3, № 4. С. 345–363. (На англ. яз., реферат на русском)
https://doi.org/10.30730/2541-8912.2019.3.4.345–363.

Introduction

The CB-TY fault zone, TY-LS section is located in Quangninh and Langson province, Vietnam. The fault zone run in the SW-NE direction, parallel to a Red River fault zone, which located in the southern part, but it is smaller. On the satellite image, the fault zone is above 100 km long. The fault zone cut through the sedimentary rocks which determined as the age from Triassic to Cenozoic. Along the fault zone has a lot of fractures and the evidences of striation motion on fault surface. The studies of geology and geodynamics along the fault zone have been carried out from many decades of the last century [Vu Van Chinh, 2002; Le Trieu Viet, 2004].

Vu Van Chinh [Vu Van Chinh, 2002] suggested that the CB-TY fault zone formed in the late Paleozoic period and re-acted in the Mesozoic and Cenozoic. The analytical results of structural geology using the methods of analyzing the conjugate fracture system along the fault zone identified two main tectonic phases, corresponding to one early and one late phase. The early tectonic phase occurred in the late Paleogene – Miocene period, the compressive stress state with the E-W axis and the extension stress state with the N-S axis. The late tectonic phase occurred in the Pliocene – Quaternary period, the compressive stress state with the N-S axis and the extension stress state with the E-W axis. The other studies along the CB-TY fault zone is mainly considered as paleontology at the Cao Bang basin, Na Duong basin [Wysocka, 2009; Phan Dong Pha et al., 2011; Böhme et al., 2011; Böhme et al., 2013].

While, the studies of tectonic activity along the Red River fault zone, parallel to the CB-TY fault zone, which located in the southern part are considered much more by Vietnam and foreign geologists, typically, it is the study of P. Tapponnier et al. [Tapponnier et al., 1986]. He suggested that the left lateral strike-slip of the Red River fault system as the result of the India-Eurasia plate collision and determined within 30 Ma to 5.5 Ma, corresponding to the Oligocene-Miocene period, from analytical results of the seismic data in the northern part of the Red River basin [Rangin et al., 1995]. The left lateral strike-slip of the Red River fault system in the Oligocene-Miocene period also mentioned by P. Leloup et al. [Leloup et al., 1995]. The offset left-lateral motion is estimated as between 200 and 800 km [Tapponnier et al., 1990; Sun et al., 2003].

Recently, the analyzing tributaries of the Red River fault system from Quaternary alluvial fans, river valley on Landsat and SPOT satellite images, detailed topographical maps and field observation has determined right-lateral offsets of stream channels range between 150 and 700 m [Phan Trong Trinh et al., 2012]. This is the results of the compression stress field of the N-S direction; E-W extension direction caused the right lateral strike-slip along the Red River fault system and, probably, began in the Pliocene time.

The another analysis also recognized that CB-TY fault zone, which is located in the northeastern part of the Red River fault system to be the right lateral strike-slip, results from the N-S compression direction using Landsat and SPOT satellite images, aerophotographs and 1:50.000 scale topographic maps [Phan Trong Trinh et al., 2012]. The relation to dextral strike-slip motion of the Red River fault system in the episode of Pliocene-Quaternary also confirmed in study of W. Zuchiewicz et al. [Zuchiewicz et al., 2013].

Similarly, the another study also indicated that predominantly sinistral strike slip of the Red River fault system formed as a result of ENE regional compression (80°) during the Oligocene-Miocene period and dextral strike slip of the Red River fault system formed as a result of NNW regional compression 330–350° during the Pliocene-Quaternary time [Kasatkin et al., 2014].

In this study, using the evidence of striation on the fault surface, the authors continue to make clearly tectonic phases along CB-TY fault zone, TY-LS section (Fig. 1).

Studying of thermal springs in Vietnam has begun only 10 years ago. The main attention is paid to the springs located in the central and southern Vietnam whereas sources in the northwest part of the country still remain the least studied.

As a result it was counted that Vietnam has 269 geothermal sources with water temperature higher than 30 °C. Among them 140 springs belong to warm and 80 to hot [Nguen Thac Cuong et al., 2005].

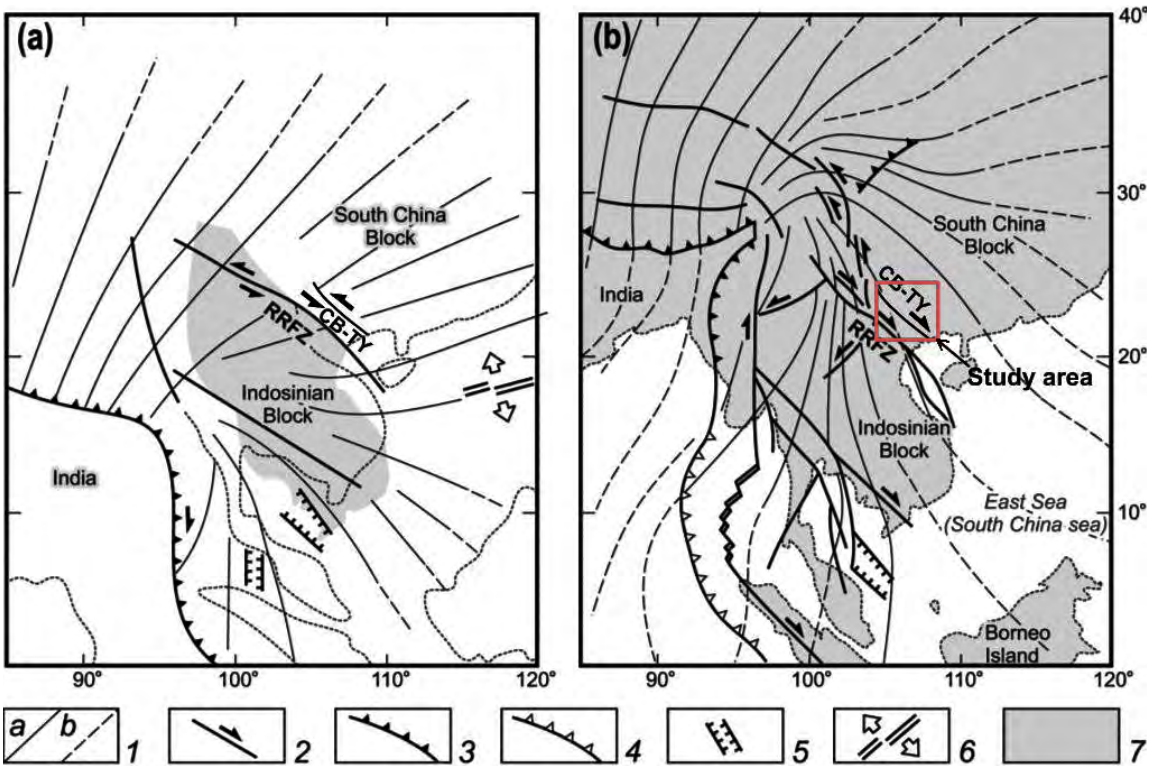

Fig. 1. Trajectories of the maximum compressive stress within the Indochina Peninsula from Pliocene to the present time [Kasatkin et al., 2014] modified from Huchon (1994).
(1) trajectories of the maximum compressive stress are directly related to the Indo-Eurasian plate collision (a) and its far-field effects (b); (2) faults and directions of displacement (arrows); (3) zone of continental collision; (4) subduction zone; (5) extension structures; (6) spreading zones; (7) current position of the land; Red River Fault System (RRFS); Cao Bang – Tien Yen fault (CB-TY).

In the northwest part of Vietnam about 79 hot springs are located which make 29.4 % of all thermal resources of the country. Thermal waters in this area have temperature on average 35–38 °C and belong to warm and moderately warm [Nguen Thac Cuong et al., 2005]. Thermal springs of the northwest of Vietnam are located in provinces Lai Chau, Son La, Hoa Binh, Yen Bai, Lao Cai and Phu Tho. All of them are associated with faulted zones NW-SE direction.

In April, 2016–2017 the staff of POI FEB RAS (Vladivostok) in collaboration with Institute of Marine Geology and Geophysics (IMGG VAST, Hanoi) has conducted researches on distribution of natural gases in thermal springs of northwest Vietnam and also a number of hydrological wells on Catba island in places of carbonate rock (Halonog Bay). Geological samples were sampled on the island also.

The researches have been successfully executed in full and are a part of a joint complex scientific geologic-geophysical research in the north of the South China Sea.

Data on distribution of methane, its homologs, nitrogen, carbon dioxide, helium and hydrogen in water of thermal sources of the northern Vietnam have been for the first time obtained. On the islands of Halong Bay unique geological samples are taken.

Water monitoring researches of the hydrological wells drilled in carbonate thicknesses are on Catba island. Study area is located on the site of the northeast frame of fault system of the Red River.

Material and method

Material

The geological survey is conducted at 21 locations along CB-TY fault zone, TY-LS section with the length of about 100 km. The data collected includes lithological characteristics, fracture orientation, fault orientation, stratigraphic displacement, striation on the fault surface. The location and character of the striations on the fault surface at each survey location are shown in Figure 2 and Table 1.

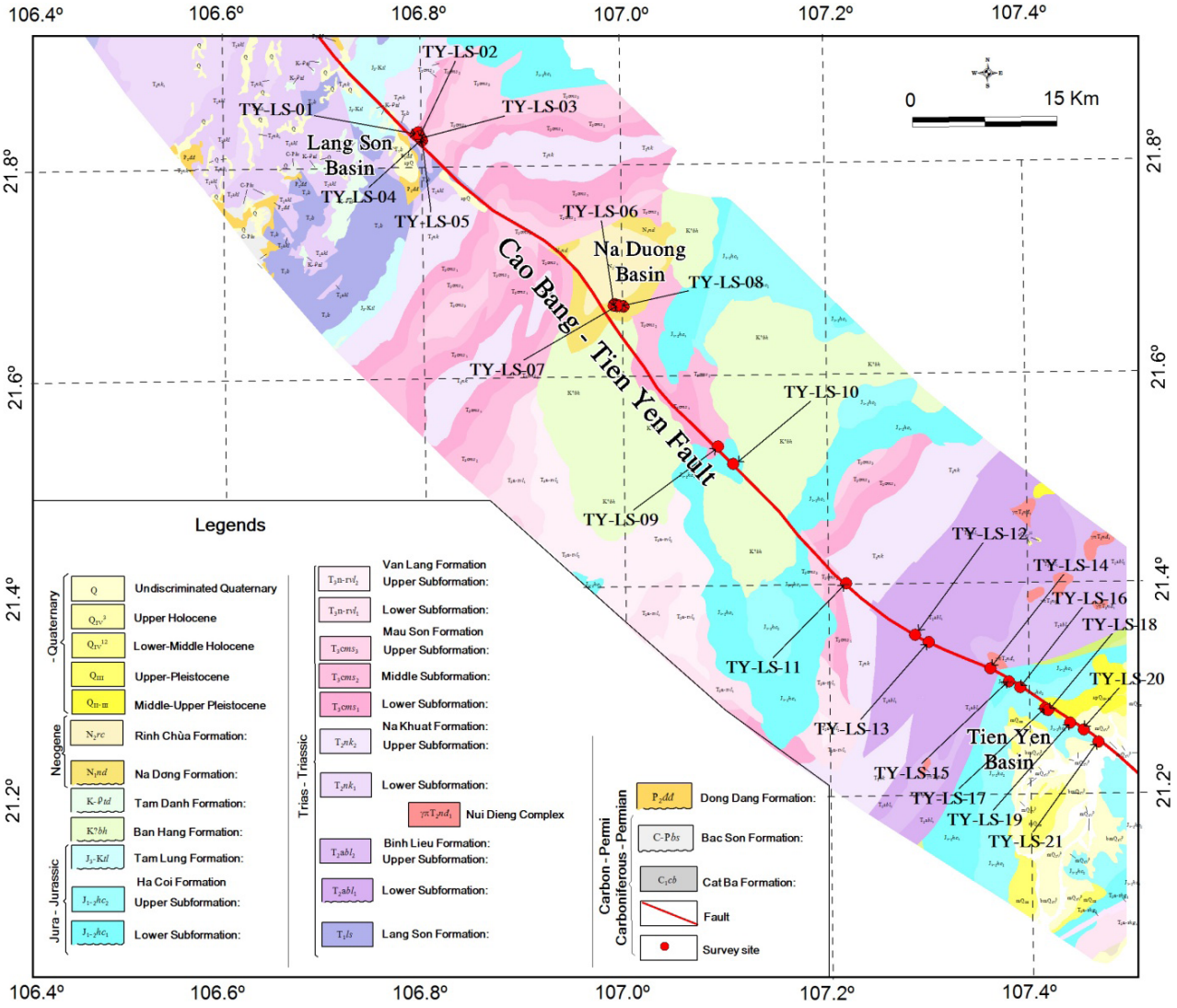

Fig. 2. Geological map, minimized from scale 1 : 200 000 and survey locations.

Table 1. **Survey locations, fault orientation and striation description**

No	Survey location index	Longitude	Latitude	Orientation	Fault description	Geological age
1	TY-LS-01	21°52’20.35"	106°46’26.82"	175/50 020/60	Left lateral strike-slip Right lateral strike-slip	T_3cms_1
2	TY-LS-02	21°52’10.77"	106°46’40.53"	105/75	Left-lateral/reverse, pitch = 30°	T_3cms_1
3	TY-LS-03	21°52’4.27"	106°46’43.5"	200/75	Right-lateral/normal, pitch = 10°	T_3cms_2
4	TY-LS-04	21°52’0.62"	106°46’47.13"	280/75	Normal	T_3cms_2
5	TY-LS-05	21°51’57.09"	106°46’48.96"	095/85	Right-lateral/normal, pitch = 50°	T_3cms_2
6	TY-LS-06	21°42’27.43"	106°58’14.37"	300/67	Normal	N_1nd
7	TY-LS-07	21°42’25.09"	106°58’25.40"	320/65	Normal	N_1nd
8	TY-LS-08	21°42’25.37"	106°58’47.49"	310/67 140/75 140/75	Right-lateral/reverse, pitch = 20° Right lateral strike-slip Right-lateral/reverse, pitch = 40°	N_1nd

No	Survey location index	Longitude	Latitude	Orientation	Fault description	Geological age
9	TY-LS-09	21°34’22.8"	107°04’24"	180/45 180/45 190/70 215/70 190/60 170/50 230/75 160/40 195/55 180/70	Normal (phase 1) Left lateral strike-slip (phase 2) Left lateral strike-slip Left lateral strike-slip Normal Right-lateral/normal, pitch = 55° Right-lateral/reverse pitch = 35° Right-lateral/normal, pitch = 40° Normal Left-lateral/normal, pitch = 30°	$T_3 cms_1$
10	TY-LS-10	21°33’23"	107°05’19"	220/65 230/40 170/64 255/52 140/50 010/85 000/70 355/80	Thrust Normal Normal Thrust Normal Right lateral strike-slip Right lateral strike-slip Normal	$J_{1-2} hc_1$
11	TY-LS-11	21°26’31"	107°12’00"	110/60	Right-lateral/normal, pitch = 35°	$T_2 nk$
12	TY-LS-12	21°23’33.10"	107°16’6.99"	052/68 070/58	Left lateral strike-slip Left lateral strike-slip	$T_2 abl_1$
13	TY-LS-13	21°23’7.19"	107°16’55.49"	065/80 090/79	Right-lateral/normal, pitch = 25° Right-lateral/normal, pitch = 10°	$T_2 abl_1$
14	TY-LS-14	21°20’49"	107°21’43"	010/87 192/87 055/72 070/70	Right lateral strike-slip Left-lateral/reverse, pitch = 30° Normal Left lateral strike-slip	$T_2 abl_1$
15	TY-LS-15	21°21’35"	107°20’36"	260/78 255/60 260/78 300/60 235/60	Right-lateral/normal, pitch = 35° Thrust Left lateral strike-slip Left-lateral/normal, pitch = 45° Thrust	$J_{1-2} hc_1$
16	TY-LS-16	21°20’29.29"	107°22’22.19"	065/60	Left-lateral/normal, pitch = 15°	$J_{1-2} hc_2$
17	TY-LS-17	21°19’17.69"	107°23’50.49"	030/75 295/80 340/70 318/72	Right-lateral/normal, pitch = 10° Left lateral strike-slip Right lateral strike-slip Left lateral strike-slip	$J_{1-2} hc_2$
18	TY-LS-18	21°19’9.50"	107°24’2.19"	075/84 075/84	Left-lateral/normal, pitch = 8° Normal	$J_{1-2} hc_2$
19	TY-LS-19	21°18’5.99"	107°25’9.89"	342/85 070/75 070/86	Left-lateral/reverse, pitch = 65° Left-lateral/normal, pitch = 58° Left-lateral/normal, pitch = 50°	$J_{1-2} hc_2$
20	TY-LS-20	21°18’1.90"	107°26’8.7"	060/80 350/77 035/85 340/77	Left-lateral/normal, pitch = 5° Right lateral strike-slip Left-lateral/normal, pitch = 12° Right lateral strike-slip	$J_{1-2} hc_2$
21	TY-LS-21	21°17’20.50"	107°27’1.40"	085/65 115/90 260/87	Right-lateral/normal, pitch = 24° Right-lateral/normal, pitch = 16° Right-lateral/normal, pitch = 10°	$J_{1-2} hc_2$

Method

To determine the overall sense of slip along the fault, we collected a fault-slip dataset from numerous discrete fault surfaces that occur along the CB-TY fault zone. A population of fault-slip data is collected by measuring the orientation of fault surfaces and associated fault striation. To interpret the population of fault-slip data and test for multiple overprinting deformations along the fault zone, we followed the graphical methods of R. Marrett and R. Allmendinger [Marett, Allmendinger, 1990]. Measurements are collected along the fault where it crops out on the slope of 4B highway, run through two districts Quangninh and Langson.

The analyses of the striation of the fault surface at each survey location are conducted as shown in Figures 3–5.

Water was sampled from wells and underground thermal sources in 0.5 l bottle. The gas is extracted by vacuum degassing for subsequent analysis in the laboratory of POI FEB RAS. About 7–9 ml of gas was extracted from each 0.5 l of water. The determination error is no more than 5 %. The gas was analyzed in the laboratory of the POI FEB RAS on the gas chromotagraph CrystalLux-4000M and portable gas chromatograph Gasochrom 2000.

Besides, the analyses also are carried out by counting the number of striation on the fault at each survey location (Fig. 5).

Results

The analyses of striation on a fault surface are conducted at 21 survey locations with 59 measurements. The analytical results showed that along the CB-TY fault zone, TY-LS section has strike-slip stress state with the compression direction of E-W, NE-SW, NW-SE and N-S, caused the left and right lateral strike – slip fault in the direction of NE-SW, NW-SE, N-S and E-W; the compression stress state of the N-S, E-W, NE-SW and NW-SE direction formed thrust fault in the E-W, N-S, NW-SE and NE-SW direction; the extension stress state of the E-W, N-S, NE-SW and NW-SE direction formed normal faults in the N-S, E-W, NE-SW and NW-SE direction. The statistical results also indicated that 05 compression stress states with the E-W direction, 04 compression stress states with the NE-SW direction, 10 compression stress states with the NW-SE direction; 02 compression stress states caused tectonic inversion of the fault in the E-W direction, 01 compression stress state caused tectonic inversion of the fault with the NE-SW direction, 01 compression stress state caused tectonic inversion of the fault with the NW-SE direction and 02 compression stress states caused tectonic inversion of the fault with the N-S direction; 14 extension stress states: 02 with the E-W direction and 02 with the N-S direction; 06 with the NE-SW direction and 04 with the NW-SE direction.

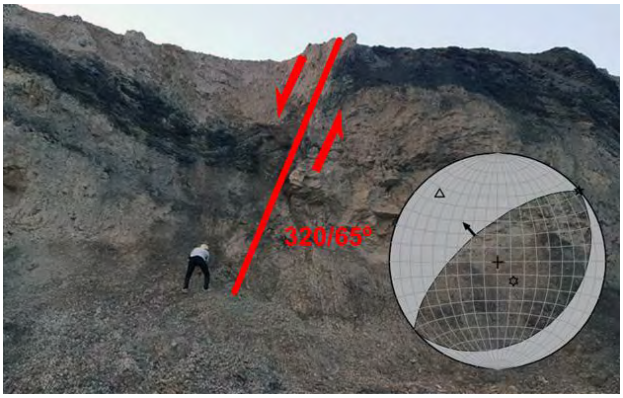

Fig. 3. Normal fault with the orientation 320/65 at survey location TY-LS-07. The analytical result determined the stress state: Sigma 1: 141/70; Sigma 2: 050/01; Sigma 3: 319/20.

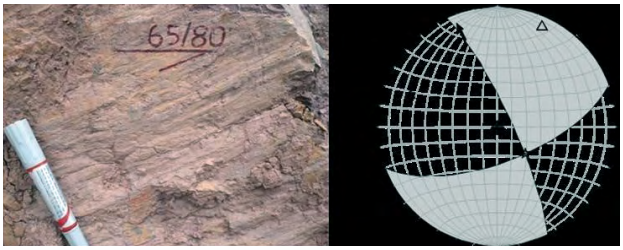

Fig. 4. The normal left fault with orientation 065/80 and striation pitch angle 250 at the survey location TY-LS-13. The analytical result determined the stress state: Sigma 1: 290/24; Sigma 2: 134/63; Sigma 3: 024/09.

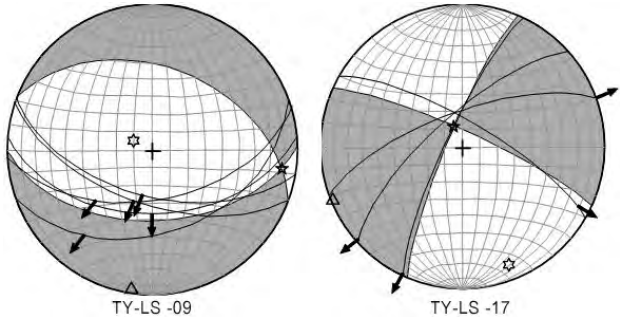

Fig. 5. The analytical result of striation on the fault surface at the survey location TY-LS-09 and TY-LS-17. The stress state determined as Sigma 1: 294/78; Sigma 2: 098/12; Sigma 3: 189/03 for TY-LS-09 and Sigma 1: 147/14; Sigma 2: 337/78; Sigma 3: 247/02 for TY-LS-17.

Compression stress state in the N-S and E-W direction

The statistical data have indicated that 04 survey locations which have a compression stress state with the E-W direction caused the left lateral strike-slip of the NW-SE fault at survey locations TY-LS-09, TY-LS-12, TY-LS-20; the right lateral strike-slip of the NE-SW fault at the survey location CB-TY-08 and the compression stress state with the N-S direction caused the right lateral strike-slip of the NW-SE fault at the survey location TY-LS-17 (Tab. 2; Fig. 6).

Table 2. **Compression stress state in the E-W and N-S direction caused the left and right lateral strike-slip of the NW-SE and NE-SW fault**

No	Survey location index	Orientation	Fault description	σ_1	σ_2	σ_3
1	TY-LS-08	140/75	Right lateral strike-slip	274/12	133/75	006/09
2	TY-LS-09	215/70	Left lateral strike-slip	082/16	220/70	349/13
3	TY-LS-12	052/68	Left lateral strike-slip	280/17	058/68	185/14
4	TY-LS-17	030/75	Right-lateral/normal, pitch = 10°	163/18	356/72	254/04
5	TY-LS-20	035/85	Left-lateral/normal, pitch = 12°	260/12	103/77	351/04

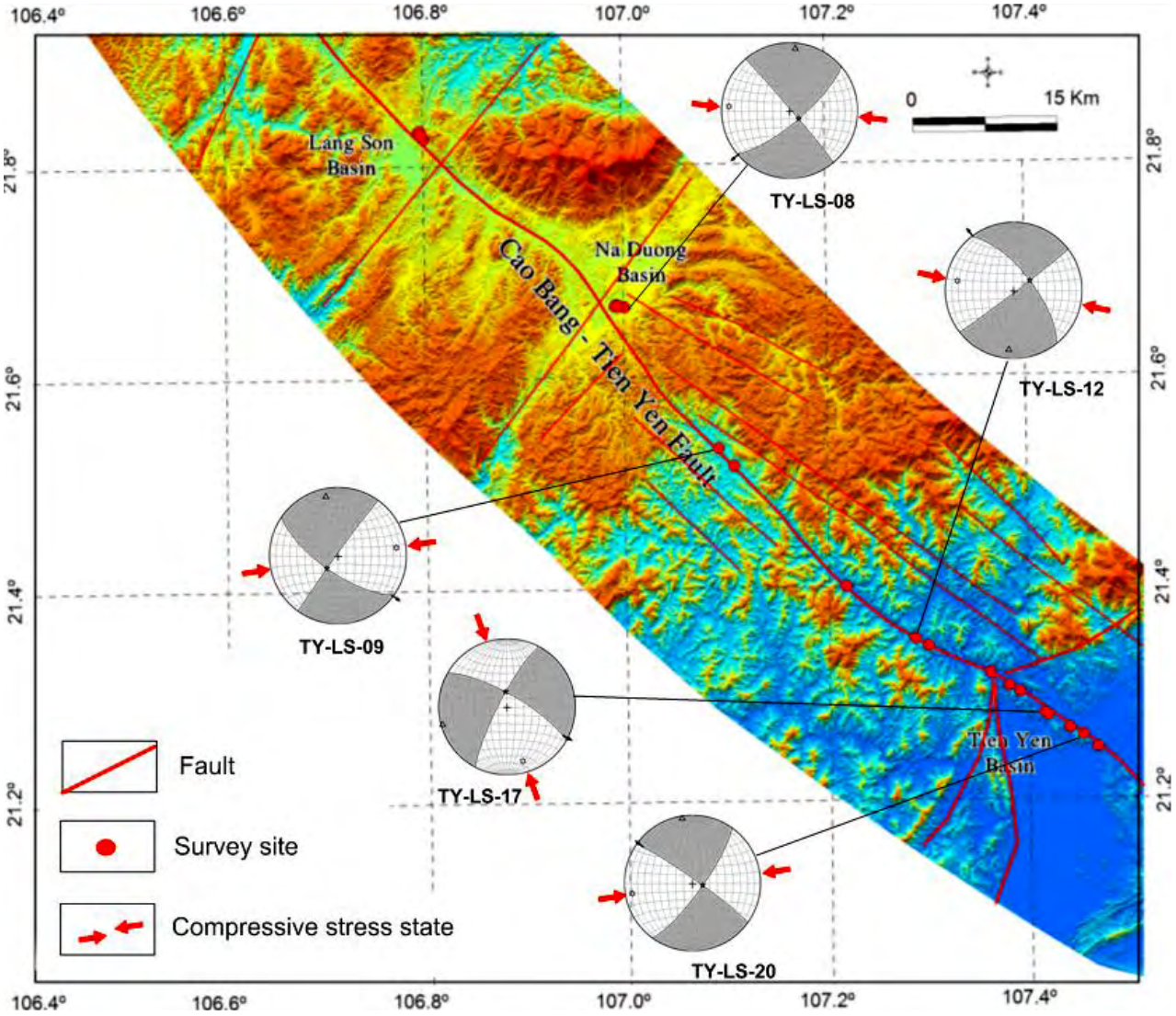

Fig. 6. Map of compression stress state in the E-W and N-S direction along CB-TY fault zone, TY-LS section.

Compression stress state in the NE-SW direction

Similarly, the statistical data also has indicated that 04 survey locations have compression stress state in the NE-SW direction, caused the left lateral strike-slip of the E-W fault at the survey locations TY-LS-01, TY-LS-03, TY-LS-09 and right lateral strike-slip of the N-S fault at the survey location TY-LS-21 (Tab. 3; Fig. 7).

Table 3. **Compression stress state in the NE-SW direction caused the left lateral strike-slip of E-W fault and the right lateral strike-slip of the N-S fault**

No	Survey location index	Orientation	Fault description	σ_1	σ_2	σ_3
1	TY-LS-01	175/50	Left lateral strike-slip	048/29	178/50	303/25
2	TY-LS-03	200/75	Right-lateral/normal, pitch = 10°	067/17	234/72	336/04
3	TY-LS-09	190/70	Left lateral strike-slip	057/16	195/70	324/12
4	TY-LS-21	260/87	Right-lateral/normal, pitch = 10°	036/10	188/80	305/04

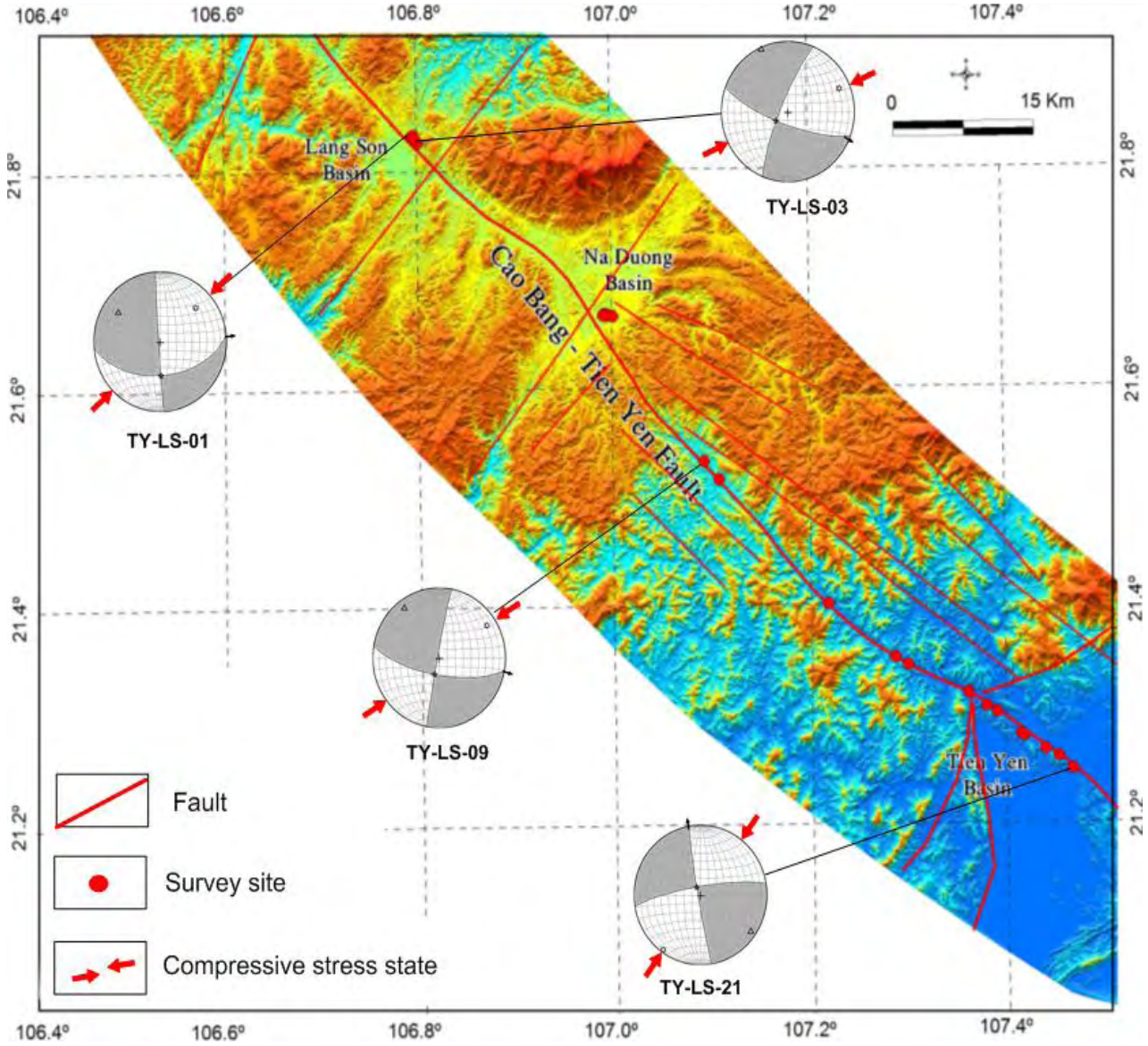

Fig. 7. Map of compression stress state in the NE-SW direction along CB-TY fault zone, TY-LS section.

Compression stress state in the NW-SE direction

The statistical data also indicated that 10 survey locations have compression stress state in the NW-SE direction, caused the right lateral strike-slip of E-W fault at the survey locations TY-LS-01, TY-LS-10, TY-LS-14, TY-LS-17, TY-LS-20; the left-lateral strike-slip of sub-longitude fault at the survey locations TY-LS-12, TY-LS-16, TY-LS-18 and left lateral strike-slip of N-S fault at the survey locations TY-LS-13, TY-LS-15 (Tab. 4; Fig. 8).

Table 4. **Compression stress state in the NW-SE direction caused the left and right lateral strike-slip of E-W fault, sub-longitude fault and N-S fault**

No	Survey location index	Orientation	Fault description	σ_1	σ_2	σ_3
1	TY-LS-01	020/60	Right lateral strike-slip	151/20	024/60	250/22
2	TY-LS-10	010/85	Right lateral strike-slip	144/04	350/84	235/03
3	TY-LS-12	070/58	Left lateral strike-slip	301/22	074/58	201/21
4	TY-LS-13	090/79	Right-lateral/normal, pitch = 10°	316/15	132/75	226/01
5	TY-LS-14	010/87	Right lateral strike-slip	145/04	337/86	235/02
6	TY-LS-15	260/78	Right-lateral/normal, pitch = 35°	126/10	268/78	035/07
7	TY-LS-16	065/60	Left-lateral/normal, pitch = 15°	298/31	092/57	201/12
8	TY-LS-17	340/70	Right lateral strike-slip	113/16	334/70	206/12
9	TY-LS-18	075/84	Left-lateral/normal, pitch = 8°	290/10	118/80	021/02
10	TY-LS-20	350/77	Right lateral strike-slip	124/11	342/77	216/07

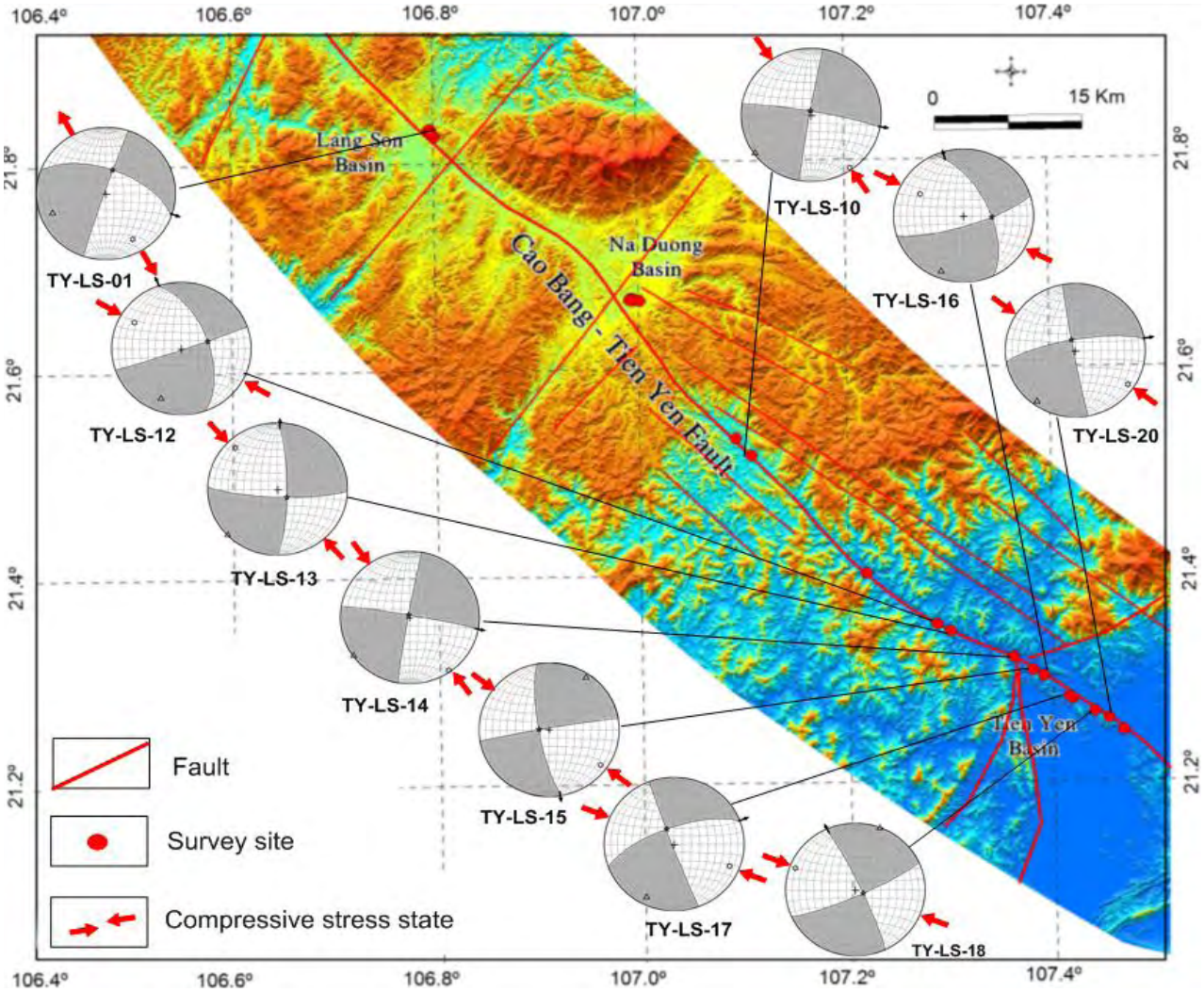

Fig. 8. Map of compression stress state in the NW-SE direction along CB-TY fault zone, TY-LS section.

Compression stress state in the E-W, N-S, NE-SW and NW-SE direction

The statistical data also indicated that compression stress state in the E-W and NE-SW direction caused the inversion of N-S fault and NE-SW at the survey locations TY-LS-08, TY-LS-15; the compression stress state in the N-S direction caused the inversion of the NW-SE and sub-latitude fault at the survey locations TY-LS-09, TY-LS-19; the compression stress state in the NE-SW direction caused the inversion of the NW-SE fault at the survey location TY-LS-10; the compression stress state in the NW-SE direction caused the inversion of NE-SW fault at the survey location TY-LS-02 (Tab. 5; Fig. 9).

Table 5. **Compression stress state in the E-W, N-S, NE-SW and NW-SE direction caused the inversion of the N-S, E-W, NW-SE and NE-SW fault**

No	Survey location index	Orientation	Fault description	σ_1	σ_2	σ_3
1	TY-LS-02	105/75	Left-lateral/reverse, pitch = 30°	142/09	038/57	239/32
2	TY-LS-08	310/67	Right-lateral/reverse, pitch = 20°	088/03	353/60	180/30
3	TY-LS-09	230/75	Right-lateral/reverse pitch = 35°	194/12	300/52	095/35
4	TY-LS-10	220/65	Thrust	219/20	310/10	041/70
5	TY-LS-15	255/60	Thrust	256/15	166/02	072/75
6	TY-LS-19	342/85	Left-lateral/reverse, pitch = 65°	003/34	254/24	137/44

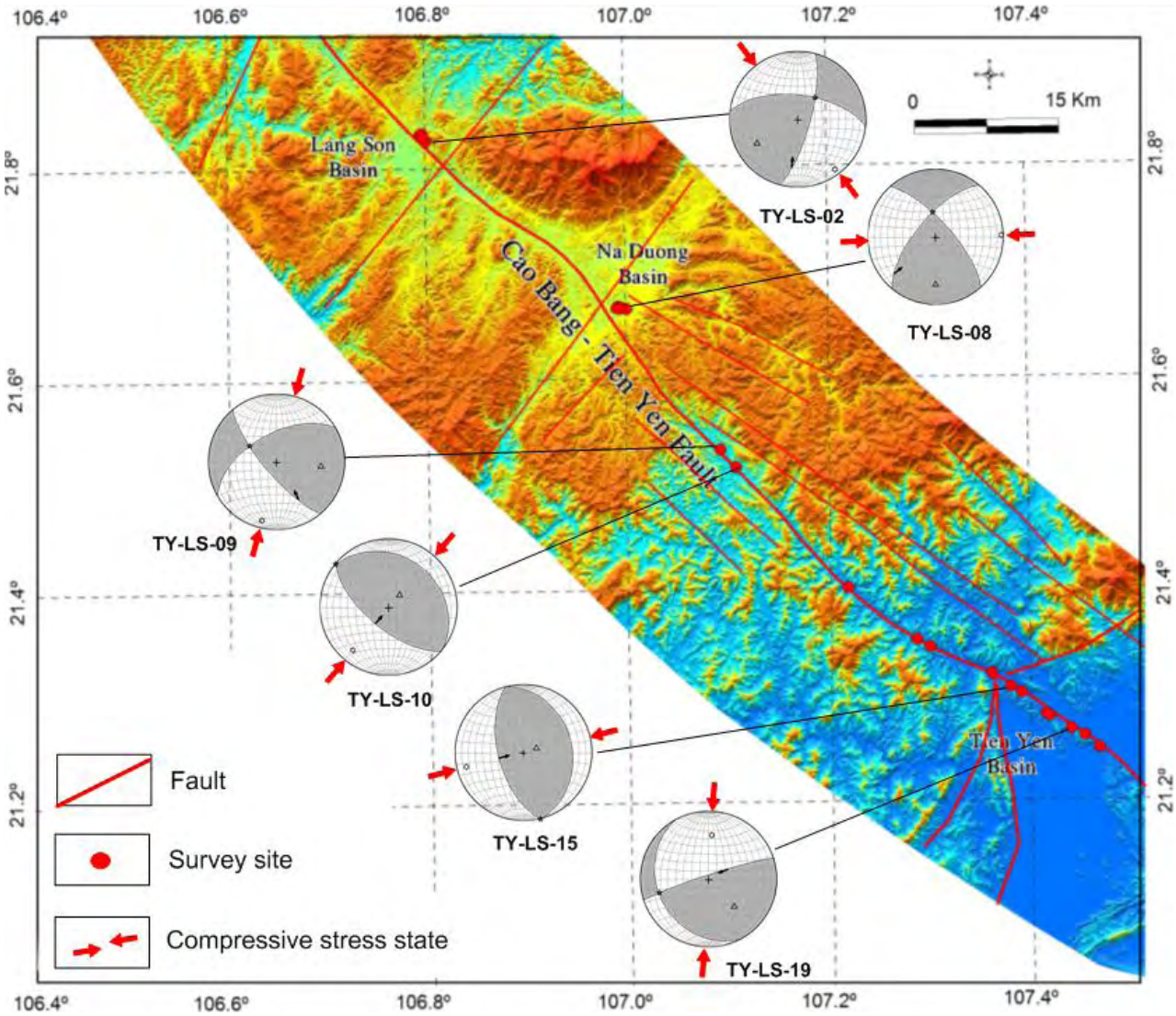

Fig. 9. Map of compression stress state in the E-W, N-S, NE-SW and NW-SE direction along CB-TY fault zone, TY-LS section.

Extension stress state in the E-W and N-S direction

The statistical data determined the extension stress state in the N-S direction formed normal faults in the E-W direction at the survey locations TY-LS-09, TY-LS-10; the extension stress state in the E-W direction formed a normal fault in the N-S direction at the survey locations TY-LS-04, TY-LS-15 (Tab. 6; Fig. 10).

Table 6. **Extension stress state in the E-W and N-S direction formed normal faults in the N-S and E-W direction**

No	Survey location index	Orientation	Fault description	σ_1	σ_2	σ_3
1	TY-LS-04	280/75	Normal	100/60	010/01	279/29
2	TY-LS-09	180/45	Normal	270/89	090/01	000/1
3	TY-LS-10	170/64	Normal	352/71	259/01	169/18
4	TY-LS-15	300/60	Left-lateral/normal, pitch = 45°	174/52	003/37	270/05

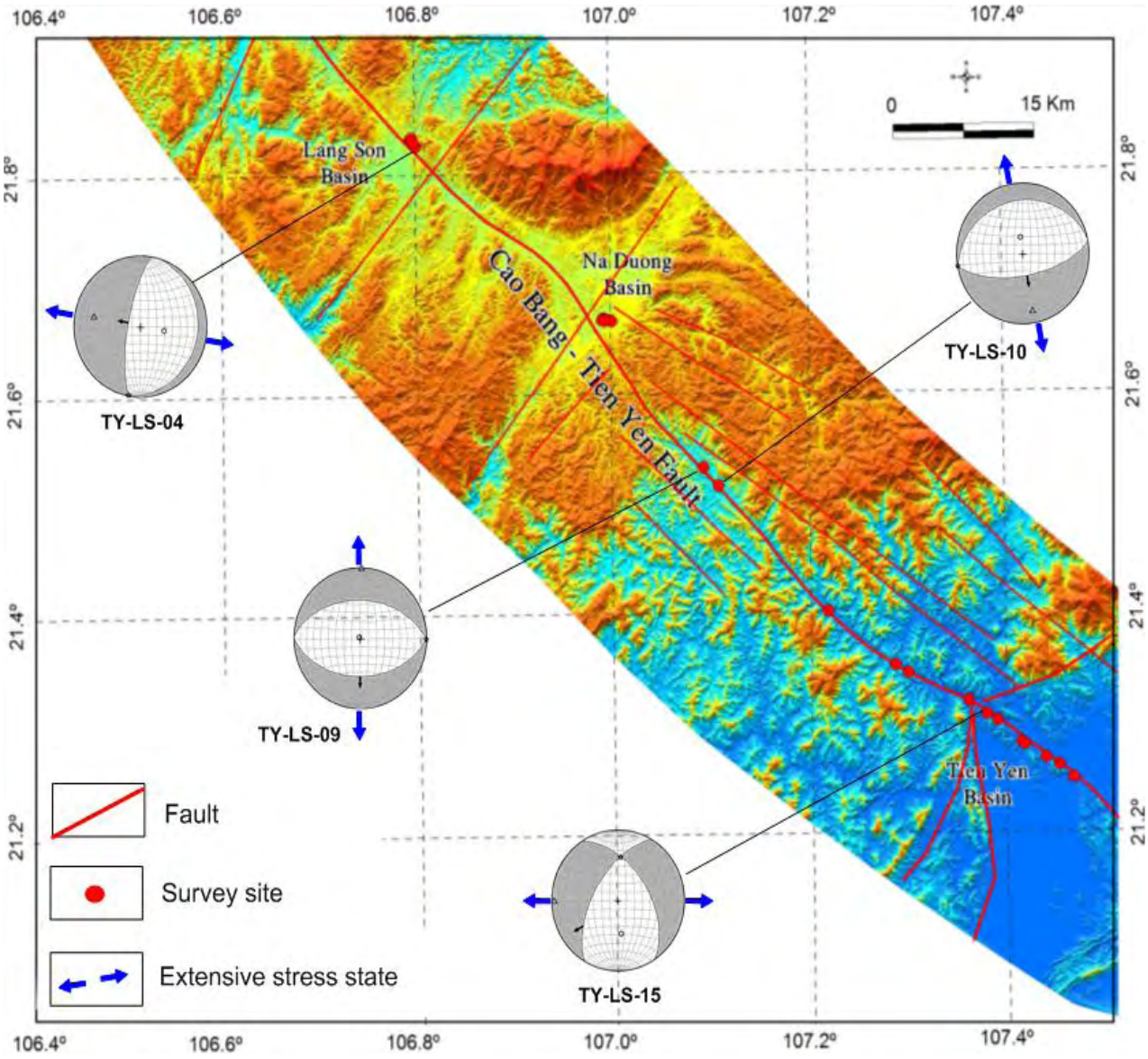

Fig. 10. Map of extension stress state in the E-W and N-S direction along CB-TY fault zone, TY-LS section.

Extension stress state in the NE-SW and NW-SE direction

The statistical data determined the extension stress state in the NE-SW direction formed the normal fault in the NW-SE direction at the survey locations TY-LS-10, TY-LS-14, TY-LS-18, TY-LS-19; the extension stress state in the NW-SE direction formed the normal fault in the NE-SW direction at the survey locations TY-LS-07, TY-LS-11, TY-LS-15, TY-LS-21 (Tab. 7; Fig. 11).

Table 7. **Extension stress state in the NE-SW and NW-SE direction formed a normal fault in the NW-SE and NE-SW direction**

No	Survey location index	Orientation	Fault description	σ_1	σ_2	σ_3
1	TY-LS-07	320/65	Normal	141/70	050/01	319/20
2	TY-LS-10	230/40	Normal	223/85	319/01	050/50
3	TY-LS-11	110/60	Right-lateral/normal, pitch = 35°	235/41	055/45	325/01
4	TY-LS-14	055/72	Normal	238/63	144/02	054/27
5	TY-LS-15	260/78	Left lateral strike-slip	036/32	187/54	297/14
6	TY-LS-18	075/84	Left-lateral/normal, pitch = 8°	246/51	155/02	064/39
7	TY-LS-19	070/75	Left-lateral/normal, pitch = 58°	285/50	150/31	046/23
8	TY-LS-21	085/65	Right-lateral/normal, pitch = 24°	215/34	037/56	306/02

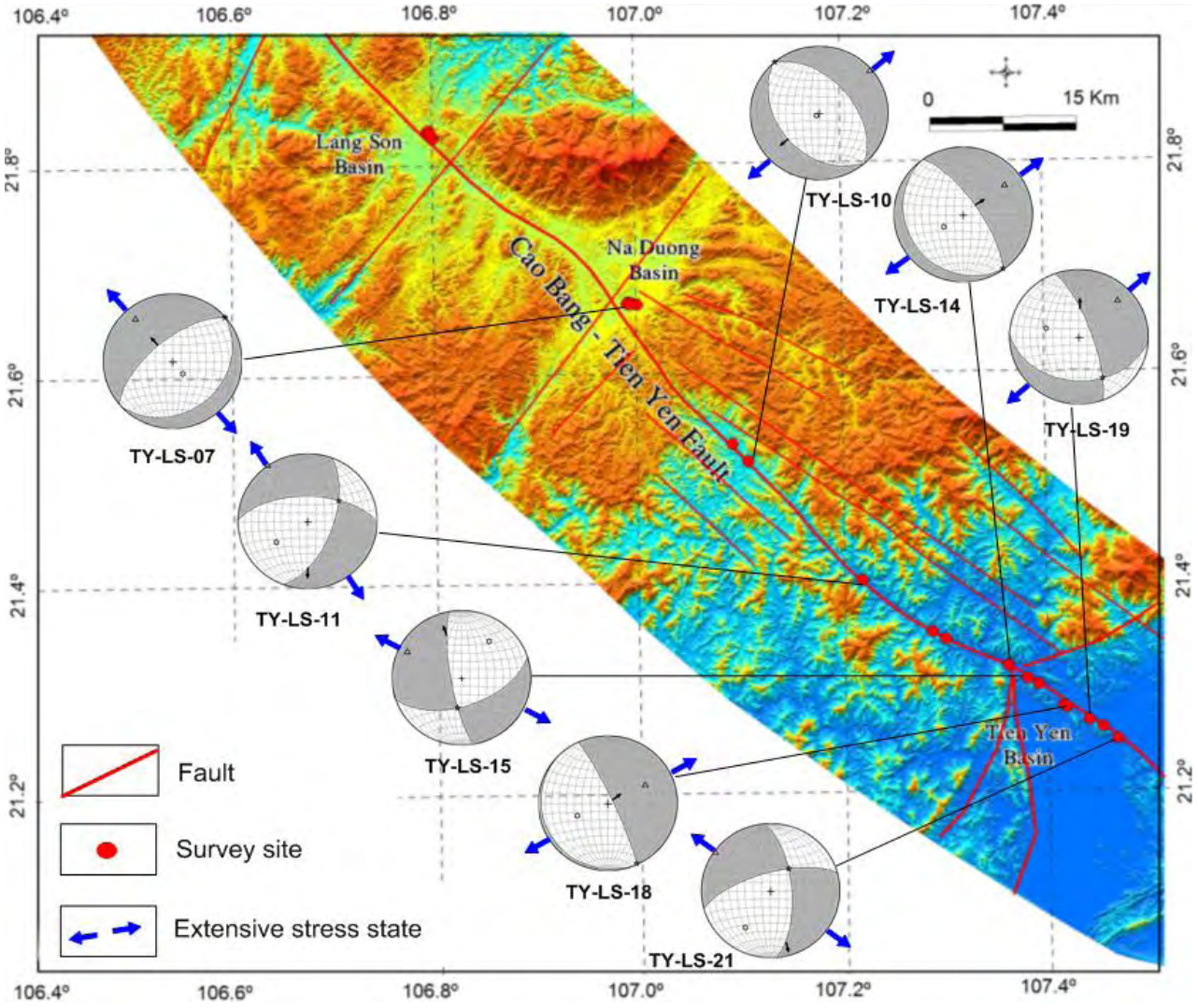

Fig. 11. Extension stress state in the NE-SW and NW-SE direction along CB-TY fault zone, TY-LS section.

Thermal springs

The most ancient carbonate formations are located in the northern Vietnam (Proterozoic –lower Cambrian). However, the main carbonate rocks in the region were created in middle Cambrian, Ordovician, Devon and Triassic. Capasity of carbonate sediments is 3000 m [Drogue et al., 2000].

The region of the northern Vietnam is tectonic active, the main active strike-slip fault zone of Southeast Asia – the Red River rift is located here. Annually in this area about 400 earthquakes are registered [Drogue et al., 2000]. Tectonic motions along the main fault zones create conditions for strengthening of deep fluid streams and opening of the new channels, especially if the region is under the influence of strong neotectonic activity.

Average air temperature near the delta of the Red River is 22–26 °C and in mountains – 15–16 °C. Thermal waters in this research we define as water, with a temperature above, than average annual temperature value of water sources on surface. In a research it is accepted that waters with a temperature over 26 °C can be considered thermal.

Thermal springs in the northern provinces of Vietnam: Hoa Binh, Phu Tho, Son La, Dien Bien, Lai Chau, Lao Kai, Yen Bai, Hai Phong were sampled. Field work included sampling water with a Niskin system batometer from thermal and mineral springs into 0.5 l bottles. Gas was extracted by vacuum method.

Water temperature, pH, mineralization, flow rate of springs were measured. 10 ml of glass containers were sampled above the source surface for subsequent calculation of methane flow into the atmosphere.

In total, more than 60 water samples were sampled and analyzed. Study object choice was based on information obtained from joint Russian-Vietnamese studies in the area of northern Vietnam in 2015–2017.

Samples were analyzed for hydrocarbon gases, N_2, O_2, CO_2, He, and H_2 (Certificate of the gasgeochemistry laboratory 1.047-18, Certificate of Rosstandart No. 41). Background gas concentrations of thermal water samples were: CH_4 – 164 nl/l, CO_2 – 21 % , ethane-butane in total – 0.34 ppm, He – 42 nl/l (3.9 ppm), H_2 – 30 nl/l (1.8 ppm) (in seawater background helium content is 8.55 ppm, hydrogen – 4.5 ppm).

The most important result of the study was the establishment of a relationship between thermal spring regime, thermogenic gas component, and geological structure of northern Vietnam.

Increased concentrations of hydrogen (5900 nl/l), helium (up to 4252 nl/l), carbon dioxide (up to 72 %), methane (up to 137776 nl/l) were found in all thermal springs within the Red River rift, that indicates geodynamic activity in the field of research and possible delivery of deep fluid through ultra-deep permeable zones.

Studies were also carried out directly at within the fault Cao Bang – Tien Yen. Researches were on hot springs in the province BaVi (delta of the Red River). The springs located to the Hanoi most closely than other hot springs of Vietnam. Water was sampled also from wells and sources in the province Hoa Binh (Kim Boi) located in 64 km to the northwest from Hanoi. On surface water has temperature 36 °C. Around the source several small reservoirs with continuously gurgling gas bubbles are located. The mineral composition of water is highly competitive with the best world brands.

Thermal waters in the northwest are associated with the fault system of NW-SE direction: Song Da, Thuan Chau, Song Hong and Song Chay faults. The springs located in the Lao Cai province are in the granite Fan Si Pan massif.

Based on tectonic data and results of the chemical composition analysis of natural gases, it is possible to claim that gases of these sources have thermogene origin. Also increased content of helium and hydrogen speaks about activity of geological structures within which sources are located. All samples contain impurity of heavy hydrocarbon gases, generally propane and butane (Tab. 8).

In case of major earthquakes, seismotectonic activation there is an increase in helium content in the thermal spring water in reference to the background value for the region. Compared to the data obtained in the tectonically active area of the Red River rift, it can be argued that the increase in the level of helium and hydrogen in the thermal spring water is a response to seismic activity and indicates gas flow from deep sources.

Table 8. **Distribution of natural gases in thermal sources of northern Vietnam by sampling results of 2016–2019**

No	Place	T water, °C	CH_4, nl/l	C_2H_4, nl/l	C_2H_6, nl/l	C_3H_8, nl/l	O_2+Ar, %	N_2, %	CO_2, %	He, nl/l	H_2, nl/l	Flow, mkmol* m^2/day
2019												
1	Hoa Binh	22.2	2153	4.3	55.9	0	4.9	48.5	42.2	52	5907	593
2	Hoa Binh	22.7	245	1	0	0	19.2	77.0	0.4	207	4077	
3	Kim Boi	35.6	84	2.2	199.7	0.28	8.5	80.1	6.4	78	1585	54
4	Kim Boi	35.6	930	3.7	211	1.72	9.2	74.5	12	34	1591	90
5	Hoa Binh city	24.4	786	1.8	0	0	15.3	63.0	18	1828	130	61
6	Phu Tho	24.9	2346	2.3	55	0.73	3.2	55.5	36.7	4253	92	197
7	Phu Tho	43.7	5042	1.2	244	0.56	7.2	75.7	12.6	140	2053	442
8	Phu Tho	22.8	218	3.2	60	0	2.9	40.7	51.5	30	718	16
9	Phu Tho	23.4	176	12.2	116.4	0	17	69.0	10.1	26	38	11
10	Phu Yen, Son La	41.5	2655	9.2	128.2	0.32	20	75.9	0.1	933	438	103
11	Son La	37.6	163	2.5	172.5	0.22	19.5	76.3	0.12	42	3.2	–
12	Dien Bien	22.1	915	1.6	90.5	0	20.1	75.9	0.01	–	–	–
13	Uba Hot Spring	84	137766	8.1	20099	12.75	20	75.6	0.01	726	29.4	22141
14	Lai Chau	34.2	1380	1.7	2000	1.47	7.3	69.3	17.8	106	2.1	11
15	Lao Cai	34.1	1839	1.8	645	0.51	7.2	66.2	21.9	152	62	59
16	Yen Bai	42	8576	1.5	271	0.34	7.3	62.0	25.8	2726	350	197
2017												
17	Sapa	21	96	1,09	0	0	19.4	75.7	0.38	84	58	–
18	Sapa	29	34	0,46	0	0	18.7	74.9	2.79	76	45	–
19	Sapa	38	142	3,14	0	0	18.6	63.8	0.53	63	52	–
20	Sapa	23	9985	8,36	0	0	24.1	74.6	4.83	85	21	–
21	Sapa	37	1152	0,62	0	0	21.3	69.9	0.48	105	30	–
22	Sapa	32	94	0,49	0	0	25.2	68.9	2.48	114	60	–
2016												
23	BaVi	33	0,12	0	0	0,002	18.04	75.7	9.11	37	28	–
24	BaVi	32	1,15	0	0	0	5.85	40.4	58.2	376	32	–
25	KimBoi	36	0,21	0,01	0	0,001	30.1	71.9	0.51	802	74	–
26	KimBoi	35	0,03	0	0	0,002	26.6	62.9	0.09	70	23	–
27	KimBoi	36	0,03	0	0	0,002	24.8	62.3	2.53	125	31	–
28	KimBoi	34	0,04	–	0	0	11.8	42.3	45.7	91	28	–

Note. The analysis is made by N.S. Syrbu, D.A. Shvalov. «–» gas component is not detected or its content is below the device detection limit (for heavy hydrocarbons – 10^{-5}).

The increased content of methane to 9985 nl/l is found in springs in the northwest near Sapa at the height from 1000 to 1300 m. The maximum concentration of methane is found in Dien Bien province located in the Dien Bien-Lai Chau active fault impact zone (up to 137766 nl/l).

The researches of thermal springs are of great importance in aspect of search of oil and gas, genesis identification of natural gases. Thermal springs of northern Vietnam need further detailed studying. However, because of hard to reach most of them, further expeditions need thorough training, the help and assistance of the Vietnamese side.

Discussions

The analytical results of 59 striations on the fault surface at 21 survey locations along CB-TY fault zone, TY-LS section determined the stress states which caused the strike-lip, inversion and extension of the faults with E-W, N-S, NE-SW and NW-SE direction. The summarized information in detail of stress state and their movement is recorded in Table 9.

The statistic results of stress state in the Table 8 showed that, the number of survey locations caused the compression stress state with the strike-slip fault in the NW-SE direction is maximum and reduce slowly under the E-W and NE-SW direction; the number of survey locations has extension stress state which caused the normal fault NW-SE and NE-SW direction is quite even, corresponding to the number of survey locations with the compression stress state in the NE-SW and NW-SE direction.

The presence of numerous survey locations caused the compression stress states in the E-W, N-S, NE-SW and NW-SE direction, reflecting the specific information of the tectonic activity phases. Each tectonic activity phase inside the Earth's crust usually leaves the specific evidences. The combination of the other analytical results such as paleontology, stratigraphy, petrology, etc. will be the basis for determining the time, dividing the tectonic activity phase and re-building the tectonic evolution.

Some analytical results of previous studies suggested that within the CB-TY fault zone has two major periods of tectonic activity which occurred in the Cenozoic [Vu Van Chinh, 2002; Pubellier et al., 2003]. The first is the left lateral strike-slip fault in the NW-SE direction (Red River fault zone and CB-TY fault zone) within the Oligocene-Late Miocene period, due to the impact

Table 9. **Summary of stress state at survey locations along CB-TY fault zone, TY-LS section**

No	Stress state direction	Survey location index	Fault description
1	E-W	TY-LS-09, 12, 20 TY-LS-08	Left lateral strike-slip of the NW-SE Left lateral strike-slip of the NE-SW
2	N-S	TY-LS-17	Right lateral strike-slip of the NW-SE
3	NE-SW	TY-LS-01, 03, 09 TY-LS-21	Left lateral strike-slip of the E-W Right lateral strike-slip of the N-S
4	NW-SE	TY-LS-01, 10, 14, 17, 20 TY-LS-12, 16, 18 TY-LS-13, 15	Right lateral strike-slip of the E-W Left lateral strike-slip of the NW-SE Left lateral strike-slip of the N-S
5	E-W	TY-LS-08 TY-LS-15	Left-lateral/reverse of the NE-SW fault Reverse of the N-S fault
6	N-S	TY-LS-09	Left-lateral/reverse of the NW-SE fault
7	NE-SW	TY-LS-10	Reverse of the NW-SE fault
8	NW-SE	TY-LS-02	Right-lateral/reverse of the NE-SW fault
9	N-S	TY-LS-09, 10	Normal of the E-W
10	E-W	TY-LS-04, 15	Normal of the N-S
11	NE-SW	TY-LS-10, 14, 18, 19	Normal of the NW-SE
12	NW-SE	TY-LS-07, 11, 15, 21	Normal of the NE-SW

of the compression stress state in the E-W direction [Vu Van Chinh, 2002; Pubellier et al., 2003; Nguyen Quoc Cuong et al., 2013; Kasatkin et al., 2014] and the right lateral strike-slip fault in the NW-SE direction, due to impact of the compression stress state in the N-S direction [Lacassin et al., 1994; Vu Van Chinh, 2002; Pubellier et al., 2003; Phan Trong Trinh et al., 2012; Zuchiewicz et al., 2013; Nguyen Quoc Cuong et al., 2013; Kasatkin et al., 2014; Michael, Phung Van Phach, 2015].

In order to analyze and determine the stress state of the tectonic activity phases at the survey locations and the separation of these phases is based on geological events such as the formation of sedimentary basins along the CB-TY fault zone and other tectonic activities in the vicinity of the northern Red River basin which are located in the southern part of the CB-TY fault zone (Fig. 12).

If we consider the compression stress state with the E-W direction occurred in the Oligocene-Miocene period, caused the left lateral strike-slip of the NW-SE fault [Vu Van Chinh, 2002] and the formation of the Cao Bang pull-apart basin which are deposited by Cenozoic sediments, the extension of the NE-SW direction in Na Duong sedimentary basin at the survey location CB-TY-07 may be also considered as the coincidence of the compression stress state in the NE-NW direction in the northern part of Red River sedimentary basin, caused the tectonic inversion here during the Mid-Late Miocene [Nguyen Giang Vu, 2003]. Next, it is the compression stress state in the N-S direction caused the right lateral strike-slip of the NW-SE fault zone during Pliocene-present [Lacassin et al., 1994; Vu Van Chinh, 2002; Pubellier et al., 2003; Phan Trong Trinh et al., 2012; Zuchiewicz et al., 2013; Nguyen Quoc Cuong et al., 2013; Kasatkin et al., 2014; Michael, Phung Van Phach, 2015]. The compression stress state caused the right lateral strike-slip with the numerous of the NW-SE direction at the survey locations along CB-TY fault zone, LS-TY section within study area can occur before the Cenozoic period of three compression directions above, such as: E-W, NE-SW and N-S. Because the striations measured on the fault surface are mostly presence in Triassic and Jurassic age and it did not see in younger rocks at the survey locations along the fault zone (Fig. 2; Tab. 1). The fracture orientation in this direction at some survey locations along the fault zone is shown in Figure 13.

Besides, the analytical results of fracture orientation at the survey locations in the sedimentary rocks O-S of the Coto formation, on the Coto-Thanhlan islands which are located in the southeastern part of the CB-TY fault zone also indicates that they have main direction NW-SE.

With the analytical results above, tectonic activity phases along CB-TY fault zone, TY-LS section can be divided into the phases, corresponding to the tectonic activity stages, follow in order of: 1) NW-SE; 2) E-W; 3) NE-SW and 4) N-S.

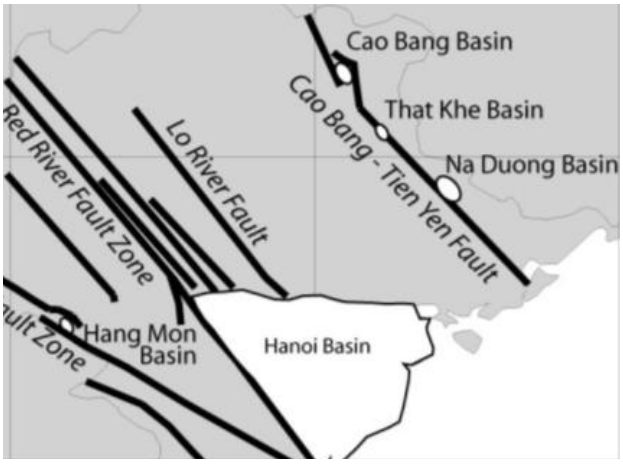

Fig. 12. Major fault systems in the northern part, Vietnam [Böhme et al., 2011].

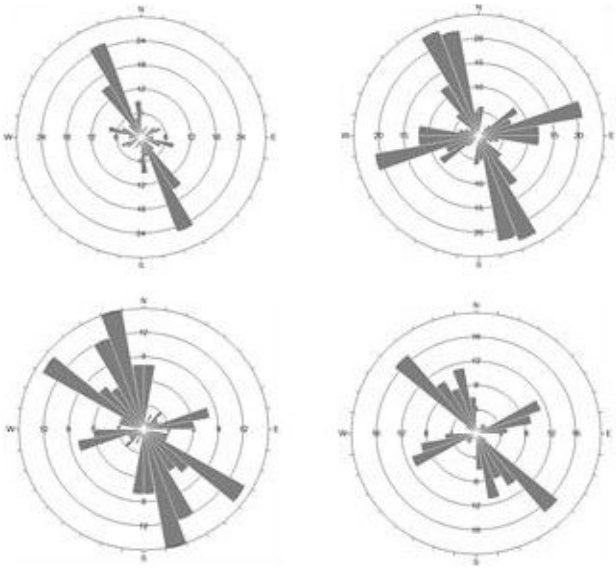

Fig. 13. Fracture orientation contour in the NW-SE, NE-SW and E-W direction measured in the sediment of Triassic and Jurassic age.

Conclusions

The analytical results of 59 striations on the fault surface at 21 survey locations along the CB-TY fault zone, TY-LS section, about 100 km long determined the strike-slip fault with the compression stress state of the E-W, NE-SW, NW-SE and N-S direction; the compression stress state of the E-W, N-S, NE-SW and NW-SE direction caused the inversion of the N-S, E-W, NW-SE and NE-SW fault; the extension stress state of the E-W, N-S, NE-SW and NW-SE direction caused normal slip of the N-S, E-W, NW-SE and NE-SW fault. The statistical results have indicated that there are 05 compression stress states in the E-W direction, 04 compression stress states in the NE-SW direction, 10 compression stress states of the NW-SE direction; 06 compression stresse states caused the tectonic inversion of 02 the E-W direction, 01 compression stress states in the NE-SW direction, 01 compression stress states in the NW-SE direction and 02 compression stress states in the N-S direction; 14 extension stress states, with 02 in the E-W direction, 02 in the N-S direction, 06 in the NE-SW direction and 04 in the NW-SE direction.

The analytical results and data from the field survey together the comparison of previous studies, this study area indicated that there are four the main tectonic phases which are arranged in the order: 1) NW-SE; 2) E-W; 3) NE-SW and 4) N-S. In particular, the first compression phase NW-SE severely destroyed the old rocks, Jurassic age and earlier, found at most of the survey locations along the CB-TY fault zone, TY-LS section will occur before the Cenozoic and Jurassic period; the second compression phase E-W occurred during the Cenozoic period, caused the left displacement of the Red River fault zone in the Oligocene-Miocene period and the left displacement along the CB-TY fault zone formed the Neogen sedimentary basins: Cao Bang, That Khe, Lang Son, Na Duong; the third compression phase NE-SW occurred during the Mid-Late Miocene, caused the tectonic inversion of NW-SW fault in the northern part of the Red River sedimentary basin which are located in the southeast of the CB-TY fault zone; the final compression phase N-S occurred during the Pliocene-Quaternary period, caused the right motion along the CB-TY fault zone and the Red River fault zone.

The major factors defining vertical or subvertical migration of gas components of the non-microbial nature are: tectonic faults, structures of extrusion, anticlinal folds complicated by disjunctive dislocation and shifts of geological structures.

The northern Vietnam is seismically active. Displacements along the main fault zones contribute to increased permeability, facilitate the advance of heat and thermogenic gases to the surface.

Thermal waters in the northwest Vietnam are associated with active fault zones. The seismotectonic activity of the region influences on their mode and gas chemical composition. Gases of the studied thermal springs have thermogene origin.

Acknowledgements

This research is supported by by the Project of "Research on the application of Block Theory to assess the risk of slope failure along the highway. Case study from km 0 to km 80 on the 3B highway", Code: TNMT.2018.03.18 of Ministry of Natural Resources and Environment, within the time 2018–2020.

The paper is financially supported by the Project of Vietnam Academy of Science and Technology (Code: VAST05.02/15-16), and partially by VAST and FEB RAS Gasgeochemical fields and CH_4/CO_2 fluxes in the Northern and Central Vietnam and its shelf: study of lithosphere, hydrosphere and atmosphere interaction (Code: VAST18-006 / QTRU02.01/18-19).

The research is supported by the RFBR (20-35-70014) "Interrelation of geosogeochemical fields, tectonics, geodynamic situation and oil and gas bearing potential, which determine geologic and hydrocarbon potential of the North Vietnam".

References

1. Böhme M., Prieto J., Schneider S., Nguyen Viet Hung, Do Duc Quang, Dang Ngoc Tran. **2011**. The Cenozoic on-shore basins of Northern Vietnam: Biostratigraphy, vertebrate and invertebrate faunas. *Journal of Asian Earth Sciences*. 40(2): 672–687. https://doi.org/10.1016/j.jseaes.2010.11.002

2. Böhme M., Aiglstorfer M., Antoine Pierre-Olivier, Appel E., Havlik Ph., Metais G., Laq The Phuc, Schneider S., Setzer F., Tapper R., Dang Ngoc Tran, Uhl D., Prieto J. **2013**. Na Duong (northern Vietnam) – an exceptional window into Eocene ecosystems from Southeast Asia. *Zitteliana*. A 53: 120–167

3. Drogue C., Cat N.N., Dazy J. **2000**. Geological factors affecting the chemical characteristics of the thermal

waters of the carbonate karstified aquifers of Northern Vietnam. *Hydrology and Earth System Sciences*. 4(2): 332–340. https://doi.org/10.5194/hess-4-332-2000

4. Huchon P., Le Pishon X., Rangin C. **1994**. Indochina Peninsula and the collision of India and Eurasia. *Geology*. 22(1): 27–30. https://doi.org/10.1130/0091-7613(1994)022<0027:ipatco>2.3.co;2

5. Kasatkin S.A., Golozubov V.V., Phung Van Phach, Le Duc Anh. **2014**. Evidences of Cenozoic strike-slip dislocations of the Red River Fault System in Paleozoic Carbonate Strata of Cat Ba Island (Northern Vietnam). *Russian Journal of Pacific Geology*. 8(3): 163–176

6. Lacassin P., Tapponnier H., Leloup Ph., Phan Trong Trinh, Nguyen Trong Yem. **1994**. Morphotectonic evidence for active movement along the Red River Fault System. In: *Proceed. Inter. Seis. Haz. South. Asia*, p. 66–71.

7. Le Trieu Viet. **2004**. Structural characteristics and evolution history of Cenozoic basins along Cao Bang-Tien Yen Fault Zone. *Vietnam Journal of Earth Sciences.* 26: 633–641

8. Leloup P.H., Lacassin R., Tapponnier P., Schärer U., Dalai Z., Xiaohan L., Liangshang Z., Trinh P.T. **1995**. The Ailao Shan-Red River shear zone (Yunnan, China), Tertiary transform boundary of Indochina. *Tectonophysics*. 251(1–4): 3–84. https://doi.org/10.1016/0040-1951(95)00070-4

9. Marett R.E., Allmendinger R.W. **1990.** Kinematic analysis of fault-slip data. *Journal of Structural Geology*. 12: 973–986. https://doi.org/10.1016/0191-8141(90)90093-e

10. Michael B.W.F., Phung Van Phach. **2015.** Late Neogene structural inversion around the northern Gulf of Tonkin, Vietnam: Effects from right-lateral displacement across the Red River fault zone. *Tectonics.* 34(2): 290–212. https://doi.org/10.1002/2014TC003674

11. Nguyen Giang Vu. **2003.** Structural evolution of the block 102 and 106 Song Hong basin-implication for hydrocarbon potential. In: *Proceedings of conference on "Vietnam petroleum institute: 25 years of development and achievements"*. p. 284–309. (In Vietnamese)

12. Nguyen Thac Cuong, Giang Cao Duy, Thang Tran Trong. **2005**. General evaluation of the geothermal potential in Vietnam and the prospect of development in the near future. In: *Proceedings World Geothermal Congress*. Antalya, Turkey

13. Nguyen Quoc Cuong, Tokarski A.K., S´wierczewska A., Zuchiewicz W.A., Yêm Nguyen Trong. **2013**. Late Tertiary tectonics of the Red River Fault Zone: Structural evolution of sedimentary rocks. *Journal of Geodynamics*. 69: 31–53. https://doi.org/10.1016/j.jog.2012.05.002

14. Phan Dong Pha, Geptner A.R., Nguyen Xuan Huyen, Petrova V.V., Le Thi Nghing, Nguyen Minh Quang. **2011**. A new discovery of stromatolite fossil in sediments of the Rinh Chua formation, Na Duong basin, Lạng Son, Vietnam. *Vietnam Journal of Earth Sciences*. 33(1): 94–96. https://doi.org/10.15625/0866-7187/33/1/282

15. Phan Trong Trinh, Ngo Van Liem, Nguyen Van Huong, Hoang Quang Vinh, Bui Van Thom, Bui Thi Thao, Mai Thanh Tan, Nguyen Hoang. **2012**. Late Quaternary tectonics and seismotectonics along the Red River Fault System, North Vietnam. *Earth-Science Reviews*. 114(3–4): 224–235. https://doi.org/10.1016/j.earscirev.2012.06.008

16. Pubellier M., Rangin C., Phach P.V., Que B.C., Hung D.T., Lung Sang C.L. **2003**. The Cao Bang-Tien Yen Fault: implications on the relationships between the Red River Fault and the south China Coastal Belt. *Advances in Natural Sciences.* 4(4): 347–361

17. Rangin C., Klein M., Roques D., Le Pishon X., Trong L.V. **1995**. The Red River Fault System in the Tonkin Gulf, Vietnam. *Tectonophysics*. 243(3–4): 209–222. https://doi.org/10.1016/0040-1951(94)00207-p

18. Sun Z., Zhou D., Zhong Z., Zeng Z., Wu S. **2003**. Experimental evidence for the dynamics of the formation of the Yinggehai basin, NW South China Sea. *Tectonophysics*. 372(1–2): 41–58. https://doi.org/10.1016/s0040-1951(03)00230-0

19. Tapponnier P., Peltzer G., Armijo R. **1986**. On the mechanics of the collision between India and Asia. *Geological Society of London, Special Publications*. 19(1): 113–157. https://doi.org/10.1144/gsl.sp.1986.019.01.07

20. Tapponnier P., Lacassin R., Leloup P.H., Schärer U., Dalai Z., Xiaohan L., Liangshang Z., Jiayou Z. **1990**. The Ailao Shan/Red River metamorphic belt: Tertiary left-lateral shear between Indochina and South China. *Nature*. 343(6257): 431–437. https://doi.org/10.1038/343431a0

21. Vu Van Chinh. **2002**. Neotectonic development phases and mechanism of the Cao Bang-Tien Yen Fault. *Journal of Earth Sciences*. 22(3): 181–187. (In Vietnamese).

22. Wysocka A. **2009**. Sedimentary environments of the Neogene basins associated with the Cao Bang-Tien Yen Fault, NE Vietnam. *Acta Geologica Polonica*. 59: 45–69

23. Zuchiewicz W., Cuong Nguyen Quoc, Zasadni J., Yêm Nguyen Trong. **2013**. Late Cenozoic tectonics of the Red River Fault System, Vietnam, in the light of geomorphic studies. *Journal of Geodynamics*. 69: 11–30. https://doi.org/10.1016/j.jog.2011.10.008

About Authors

TRUONG THANH PHI, Dr, Lecturer, Department of Geology, Hanoi University of Natural Resourses and Envinronment, Hanoi; SHAKIROV Renat Bellalovich (ORCID 0000-0003-1202-0351), Dr Sci. Geology and Mineralogy, Head of Laboratory of gasgeochemistry, deputy director, SYRBU Nadezhda Sergeevna (ORCID 0000-0002-1441-6133), Cand. Sci. Geology and Mineralogy, Researcher, Laboratory of gasgeochemistry – V.I. Il`ichev Pacific Oceanological Institute, Far Eastern Branch, Russian Academy of Science (POI FEB RAS).